Direct and indirect radiative effects of sea-salt aerosols over Arabian Sea

V. Vinoj and S. K. Satheesh*

Centre for Atmospheric and Oceanic Sciences, Indian Institute of Science, Bangalore 560 012, India

Estimation of the indirect radiative effect of aerosols requires an understanding of the role of aerosols in influencing cloud properties. Several investigations have focused on the determination of the indirect effect, but most of them were confined to the anthropogenic (man-made) sulphate aerosols. Studies on the indirect effect of natural aerosols (such as sea salt) are rather few. In this article, a simple approach has been used to determine the indirect effect of sea-salt aerosols over the Arabian Sea for different seasons using long-term data available from ship-borne and island-based observations in the past. We demonstrate that the indirect radiative effect of sea-salt (natural) aerosols (at the top of the atmosphere) is as large as -7 ± 4 Wm^{-2} when compared to the direct radiative effect of -2 ± 1 Wm^{-2}, and hence cannot be ignored. These values are larger than the anthropogenic aerosol forcing ($\sim 5.0 \pm 2.5$ Wm^{-2}) reported over this region. The high variability in indirect effect from -4 Wm^{-2} to around -18 Wm^{-2} brings out the importance of natural aerosols in this region. The study also demonstrates the important role of wind speed on aerosol characteristics and hence its impact on direct and indirect radiative effects. The magnitude of indirect radiative effect (and uncertainty) is several-fold more than the direct radiative effect of sea-salt aerosols.

DETERMINATION of the radiative effects of aerosols is currently one of the challenging problems in climate research. Aerosols influence the earth's radiative balance directly by scattering incoming short-wave radiation back to space and indirectly through their influence on cloud properties[1–3]. The indirect effect is considered to be one of the largest uncertainties in current global climate models (GCMs)[3]. Accurately estimating the indirect radiative effect of aerosols requires an understanding of the role of aerosols in influencing cloud properties.

Aerosols act as cloud condensation nuclei (CCN) during the formation of clouds. An increase in aerosol concentration leads to an increase in cloud droplet number and hence increases the cloud albedo (also called as 'Twomey effect')[1]. Also, for a given water-vapour content, an increase in aerosol concentration decreases the effective cloud-droplet size and hence possibly decreases the lifetime of the clouds[1]. These changes in cloud albedo and cloud lifetime in turn influence the radiation budget of the earth. The influence of aerosols on cloud microphysics depends on several factors that are poorly understood. There have been several studies to determine the aerosol indirect effect[2–10]. However, most of these studies were focused on determining the indirect effect of anthropogenic sulphate aerosols. Studies to determine the indirect effect of natural aerosols are rather few. In this article, we have made preliminary estimates of the indirect effect of sea-salt aerosols, which is one of the major natural aerosol species, using the available database.

The study was conducted using data obtained over Arabian Sea (AS) and North Indian Ocean (NIO) region adjoining the Indian subcontinent. This region is characterized by strong monsoon phenomena, where the wind reverses its direction with season. Hence this region is influenced by winds from the continent during winter monsoon season (November–March) and from the ocean during summer monsoon season (June–September)[11]. Winds as high as 15 to 20 m s^{-1} were reported over AS during southwest monsoon season[11,12]. The persistent high wind speeds over AS during summer monsoon season produce large amount of sea-salt aerosols that in turn may influence the cloud microphysics and hence the radiative forcing. In this article the direct and indirect effect of sea-salt aerosols over AS has been estimated and discussed.

Data and approach

It has been estimated that the ocean contributes ~1000 to 2000 Tg per year of aerosol flux into the atmosphere. There have been several investigations on the dependence of sea-salt aerosols on wind speed[11,13–19]. The above investigations have revealed the relationships between wind speed and aerosol properties. Studies over oceanic regions adjoining the Indian subcontinent as part of the Indian Space Research Organization's Geosphere Biosphere Programme (ISRO–GBP), Indian Ocean Experiment (INDOEX) and the Arabian Sea Monsoon Experiment (ARMEX) have revealed a relationship of the form[18,19],

$$t_a = t_0 \exp(bU), \quad (1)$$

where t_a is the aerosol optical depth (AOD) at wind speed U, b is a coefficient called wind index and t_0 is the AOD

*For correspondence. (e-mail: satheesh@caos.iisc.ernet.in)

at wind speed $U = 0$. The higher values of b indicate stronger dependence of AOD on wind speed U.

We have used data from four locations over AS and the Indian Ocean[9,11,12]. These are (i) Minicoy (8.3°N, 73°E), an island located at the southern tip of the Lakshadweep Island chain operated as part of ISRO–GBP; (ii) ship-based measurements over tropical Indian Ocean as part of INDOEX; (iii) Kaashidhoo Climate Observatory (KCO; 4.9°N, 74.5°E), Republic of Maldives operated as part of the INDOEX and (iv) northern and central AS as part of ARMEX.

Minicoy is an island station located about 400 km away from the mainland (India) and is free from local anthropogenic and industrial activities. Therefore, aerosol characteristics over this location can be expected to be purely marine, especially during summer monsoon season[11]. Aerosol observations are being made at Minicoy since 1995, as part of ISRO–GBP. Over Minicoy, the coefficients t_0 and b were 0.25 and 0.04 respectively[11]. But these values are obtained from data covering all seasons. If we consider only the southwest monsoon season (when winds are mainly from the ocean), values of t_0 and b become 0.29 and 0.07. The coefficient b does not depend on season, whereas coefficient t_0 may depend on season. However, studies at Minicoy spanning over all seasons have shown that variation of t_0 with season is not significant (less than one standard deviation). The possible reason for this is discussed later in this section.

KCO is also an island station over the NIO located about 400 km away from the mainland (India), with similar meteorological conditions as in Minicoy. Observations of aerosols were carried out at this station as part of the INDOEX field experiments. Studies at KCO yielded coefficients 0.17 and 0.08 respectively[19,20]. At KCO also, similar to Minicoy, seasonal variation of t_0 was not significant[19].

ARMEX field experiment was conducted in the northern and central AS during the summer monsoon period (16 July–17 August 2002)[12]. The summer monsoon season of the year 2002 was conducive to take aerosol observations because of the weak monsoon and hence clear sky conditions. The data yielded coefficients t_0 and b as 0.34 and 0.016 respectively[12]. The values reported for equatorial Indian Ocean during winter monsoon season are 0.07 and 0.12 respectively[18]. This is based on data collected using ship-borne measurements.

It should be noted that the background aerosol increases towards the north. As evident from geography, this could be because of the continental influence. AS is influenced by two aerosol sources (other than the locally produced sea-salt aerosols) in different seasons; from the Indian subcontinent during winter monsoon season and from Arabian/Saharan region during summer monsoon season[11]. As such, there might exist a north-south gradient in aerosol loading irrespective of season. This explains the near invariability of the coefficient t_0 with respect to season.

Wind index b is found to increase towards the south. Equation (1) represents the enhancement of AOD in response to increase in sea-surface winds. At a marine location where major part of the aerosol is contributed by sea salt, an increase in sea salt concentration would reflect on the total optical depth at nearly the same rate. Over northern AS, sea salt is only one among the various species that contribute to composite AOD. As such, any increase in sea-salt concentration would not have a similar impact on the composite AOD. This explains the lower rate (i.e. lower value of coefficient b) at which the AOD increases in response to wind speed as the latitude increases (towards the north). The values of t_0 and b are plotted as a function of latitude in Figure 1. Circles show the observations and horizontal lines show the latitudinal extent that the ship cruises have covered. The curves represent the least square fit to the observations. Two island observations are represented as circles without horizontal bars. A close examination of these coefficients (t_0 and b) observed at the four locations described above (Figure 1) reveals a nearly exponential variation of t_0 and b with latitude. Empirical relations are derived by least-square fitting of the observations of these coefficients with latitude and the following equations (eqs (2) and (3)) are obtained. Even though four points are not sufficient to determine whether linear or exponential fit is appropriate, the rationale of using exponential fit is the following. Previous observations of AOD as a function of latitude have shown an exponential decrease as we move towards south in AS[18], and hence we used an exponential fit to t_0 as well. In the case of b, an exponential variation with latitude is obvious from Figure 1. Moreover, if we use a linear fit, we get negative values at latitudes greater than 16°N.

$$t_0(\text{lat}) = 0.079\exp(0.116*\text{lat}), \quad (2)$$

$$b(\text{lat}) = 0.132\exp(-0.135*\text{lat}). \quad (3)$$

Determination of indirect effect

Determination of indirect effect due to sea-salt aerosols involves the determination of sea salt optical depth over the region and of its role in modifying cloud microphysics.

This study thus involves three steps (following Ramanathan *et al.*)[9].

(i) Determination of optical depth due to sea-salt aerosols generated by sea-surface wind speed.

(ii) Determination of change in cloud microphysical properties due to the presence of sea-salt aerosols (using empirical relations connecting aerosols and cloud properties based on previous observations in this region).

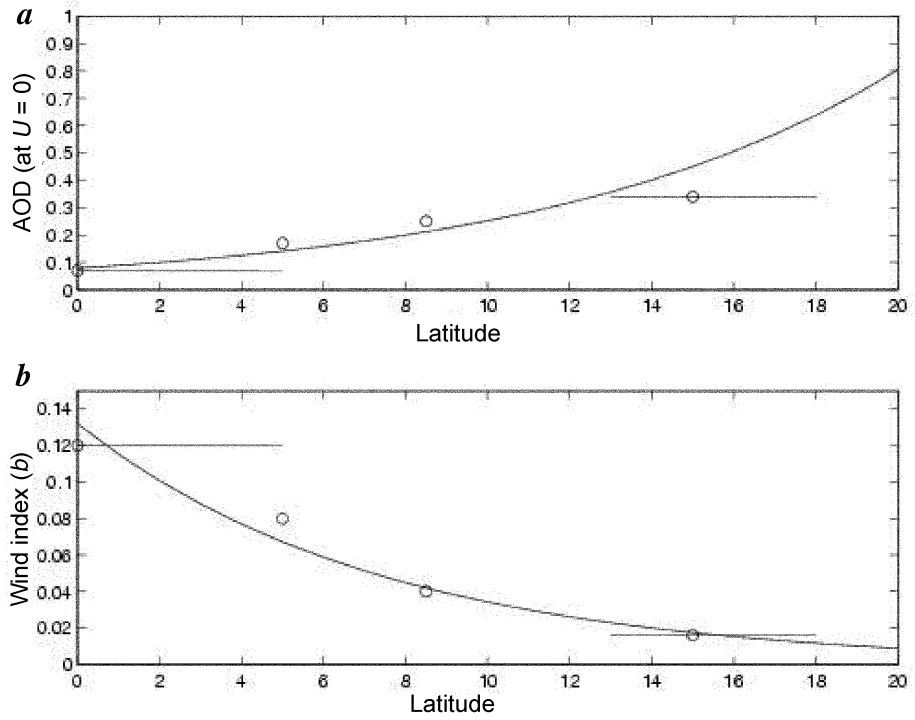

Figure 1. Variation of (***a***) t_0 and (***b***) wind index b with latitude. Horizontal bars are the latitudinal extent of the cruises.

(iii) Determination of change in cloud radiative forcing due to the presence of sea-salt aerosols (i.e. indirect radiative effect due to sea-salt aerosols).

It is well known that over the oceans, wind is the primary mechanism of production of sea-salt aerosols. Several studies have reported a direct relationship between aerosol properties and wind speed[13–18,21,22]. AOD due to sea-salt aerosols is obtained by substituting the latitude variation of the coefficients t_0 and b (eqs (2) and (3)) in eq. (1), where the values of wind speed are obtained from National Centers for Environmental Prediction (NCEP) data. The distribution of winds over AS is shown in Figure 2. The values of U used here are $2.5° \times 2.5°$ pixel values, which are averaged for the period 1995–2002. The latitudinal values of t_0 (i.e. optical depth when wind speed is zero) are subtracted from the total optical depth (eq. (1)) to get the optical depth due to wind-induced sea-salt aerosol (eqs (4) and (5)).

$$t_a(\text{lat, long, } U) = t_0(\text{lat})\exp[b(\text{lat})*U(\text{lat, long})], \quad (4)$$

$$t_{\text{sea-salt}}(\text{lat, long, } U) = t_a(\text{lat, long, } U) - t_0(\text{lat}). \quad (5)$$

There have been several studies to determine the indirect effect using data on cloud microphysical properties and aerosol parameters from aircraft[9,23–27]. These studies have demonstrated that the indirect effect due to aerosols depends on the relationships between aerosol number density (N_a), cloud droplet number density (N_c), cloud droplet effective radius (R_{eff}), cloud optical depth (t_c) and cloud albedo (A_c). Several investigators[9,25–27] have reported from observations that there exists a significant correlation between N_a and N_c. Extensive observations of aerosols and clouds (using aircraft) over AS and NIO were made during INDOEX from November 1998 to March 1999. This observational campaign brought to light several results relating to the role of aerosols in altering cloud properties[9].

The vertical distribution of aerosols over this region was inferred using lidar data as well as data from the National Center for Atmospheric Research (NCAR) C-130 aircraft, and are reported in Ramanathan *et al.*[9]. They have reported two types of typical vertical distributions; one in which the aerosol is concentrated in the boundary layer and another in which an elevated layer is observed near ~ 2 to 3 km. About two-third of the time the aerosol layer at 2–3 km was present and one-third of the time, it was concentrated in the boundary layer[9]. In this study, we have used a combination of the above two profiles (weighted average) following Ramanathan *et al.*[9].

Observations over AS and Indian Ocean during INDOEX[9,26,27] have revealed the following relationship connecting CCN number density (N_c) and N_a. From simultaneous measurements of aerosol vertical profiles and columnar optical depth, N_a at cloud level was derived.

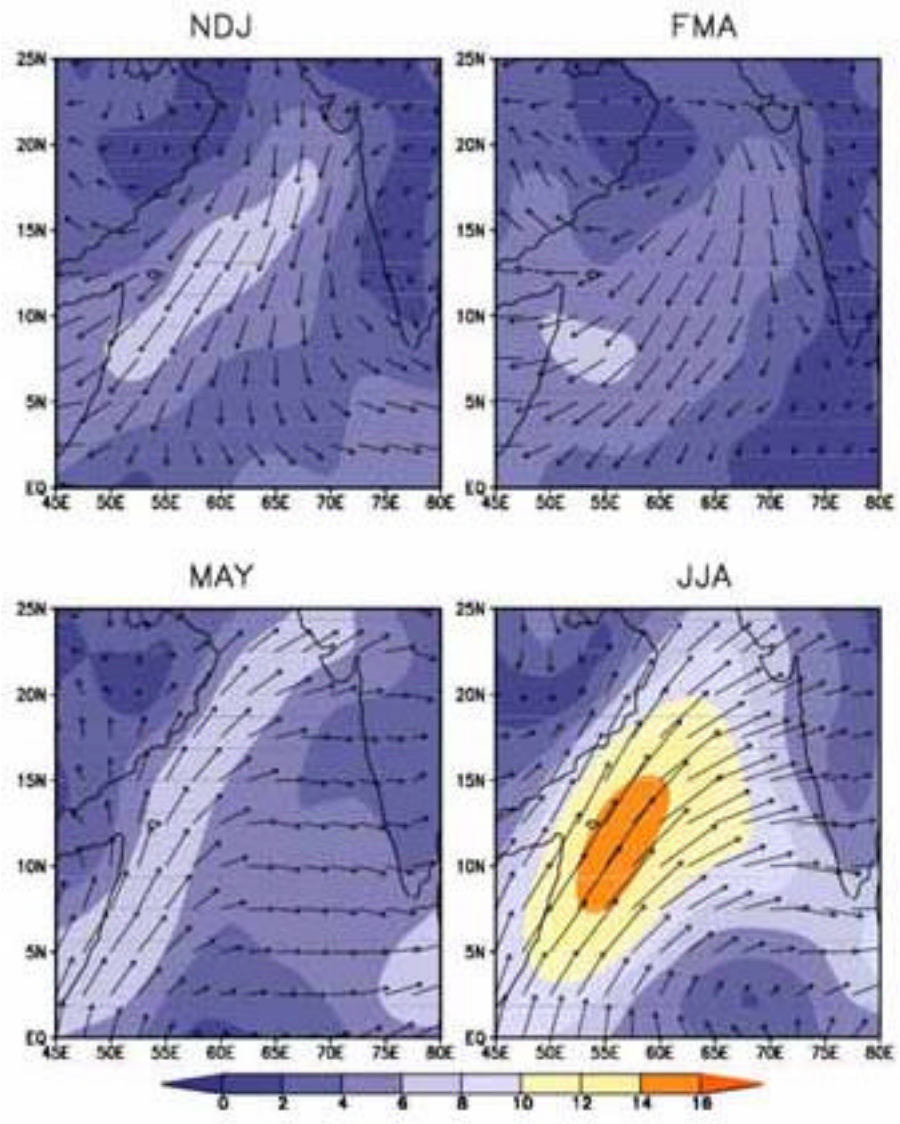

Figure 2. Seasonal wind speed and direction over Arabian Sea during NDJ (November to January), FMA (February to April), MAY (May), and JJA (June to August) respectively.

$$N_c = bN_a^n [S/0.3]^k, \quad (6)$$

where $b = 0.12$; $n = 1.25$, $k = 0.76$.

The water vapour super saturation (S) and N_a of aerosols are related by,

$$S = 0.18\exp(-0.00065N_a). \quad (7)$$

The inverse relationship between S and N_a is due to the fact that as N_a increases, more drops are nucleated thereby reducing the water vapour amount and hence, S[9].

R_{eff} is given by the expression,

$$R_{eff} = [3L/4pKN_c]^{1/3}, \quad (8)$$

where $k = 0.73$ and L is the cloud liquid-water content. The factor K accounts for the deviation from mono-disperse size distributions.

The optical depth due to cloud droplets is obtained using the relation[9,24],

$$t_{cloud} = pR_{eff}^2 Q_{ext} N_c \Delta z, \quad (9)$$

where Q_{ext} is the extinction efficiency factor ($Q_{ext} \sim 2$ as cloud droplets are much larger than the visible wavelengths), and Δz is the thickness of clouds. An average thickness of ~300 m was used in this study following observations reported during INDOEX[9]. It should be noted that the cloud thickness might be different during summer monsoon season. However, we estimate the indirect effect due to sea-salt aerosols under the same conditions for June, July and August months also, only to show the possible role of high winds during that season on the indirect effect. In actual case, the indirect effect may be still

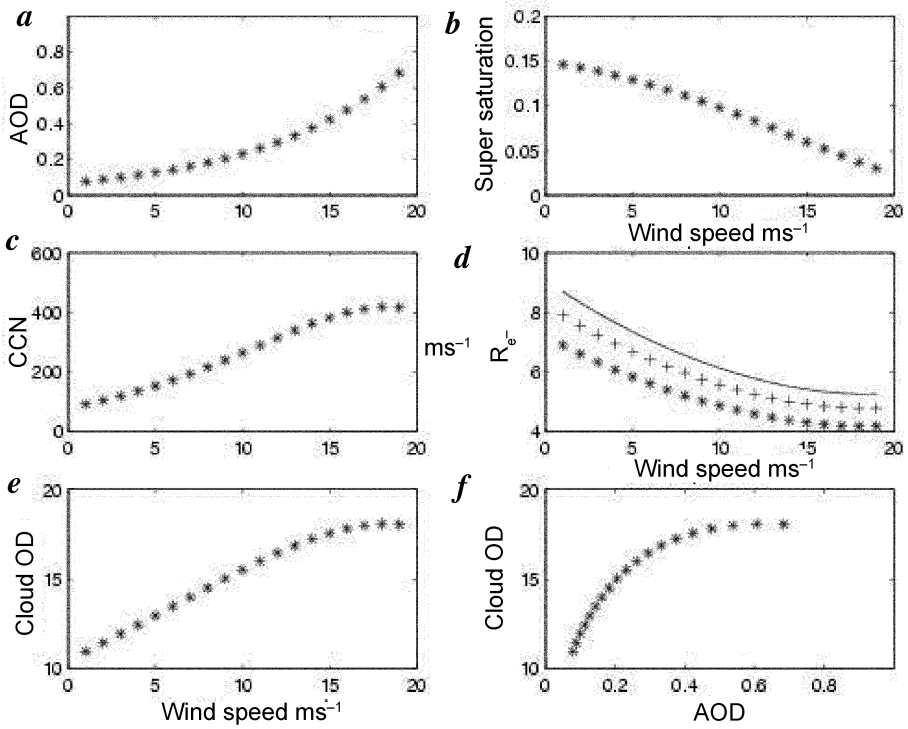

Figure 3. Variation of (***a***) AOD, (***b***) super saturation, (***c***) CCN, (***d***) R_{eff} and (***e***) cloud optical depth (COD) with wind speed, and (***f***) variation of cloud OD with AOD.

higher. Moreover, the liquid-water content will be higher during summer monsoon season and hence the indirect effect as well. The error due to this can be as high as 20%.

The variation of AOD, super saturation, CCN, cloud optical depth and R_{eff} as a function of wind speed (U) are shown in Figure 3 (derived using eqs (6)–(9)). In Figure 3, different curves in R_{eff} vs U represent the effect of liquid-water content (L). Different curves represent different L of 0.1, 0.15 and 0.2 g m^{-2} for case 1, case 2 and case 3 respectively. All the calculations we report here follow an L value of 0.15 g m^{-2} based on measurements during INDOEX[9].

The saturation of the above parameters (CCN, cloud optical depth and R_{eff}) at high wind speed is due to the fact that for a given liquid-water content in the atmosphere, an increased aerosol number due to high winds creates a deficit in water content. In other words, for a given water content, water vapour availability per aerosol is more when aerosol number density is less. The lack of availability of moisture leads to saturation of these parameters at high winds. This fact is also seen in Figure 3*f* showing the relationship between cloud optical depth and AOD.

The relation between AOD and cloud optical depth is the key in estimating aerosol indirect effect[9]. The SBDART (Santa Barbara DISORT Atmospheric Radiative Transfer) model developed by the University of Santa Barbara was used to derive the change in cloud forcing due to a change in cloud optical depth[19,28]. Thus, using the relationships between aerosol and cloud parameters as described above and shown in Figure 3, as input to the SBDART model, change in cloud forcing (indirect radiative effect) as a function of sea-salt aerosol optical depth was determined. This approach was applied to regional distribution of sea-salt optical depth, and regional distribution of indirect effect was estimated.

Results and discussion

Regional distribution of various parameters (AOD due to sea salt, AOD due to clouds, direct radiative effect and indirect radiative effect due to sea-salt aerosols) described above is shown in Figures 4 to 6. Direct radiative effect was estimated using sea-salt AODs in SBDART model. Other optical properties of sea salt required were obtained from Hess *et al.*[29]. All the figures have four panels, each representing four different seasons (NDJ, FMA, MAY and JJA). The patterns observed in the figures demonstrate the importance of the sea-surface wind speed in determining aerosol radiative effects. Figure 4 shows distribution of sea-salt AOD during four different time periods. The value of sea-salt AOD is in the range 0.01 to 0.1 during November to May. However, it exceeds 0.2 (especially over Somali region) during June to August. This high sea-salt AOD during JJA is due to high winds in the range of 15 to 20 m s^{-1} during that season (Figure 2).

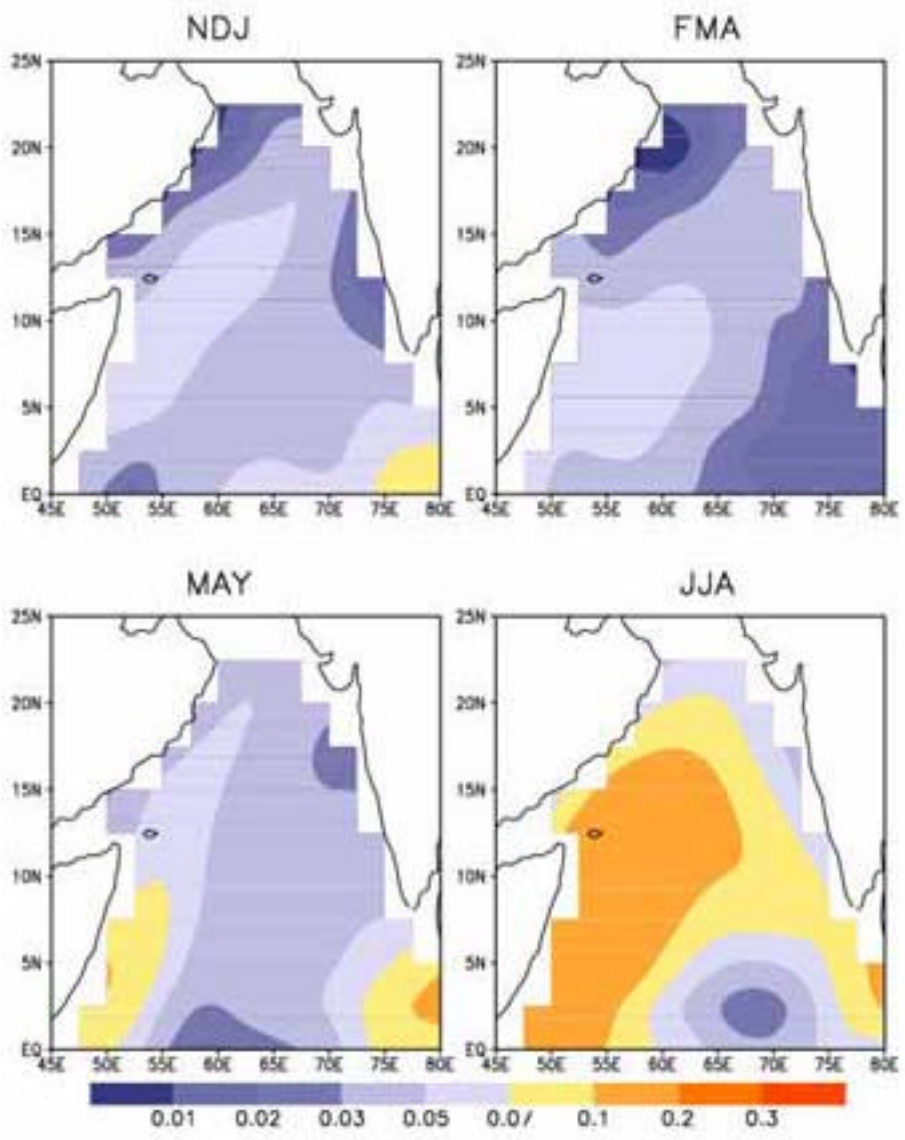

Figure 4. Optical depth due to sea-salt aerosols over Arabian Sea during NDJ (November to January), FMA (February to April), MAY (May) and JJA (June to August) respectively.

Figure 5 shows the distribution of direct radiative effect (at the top of the atmosphere) due to sea salt. The direct effect is in the range –1 to –4 Wm^{-2} during November to May, but exceeding –8 Wm^{-2} during JJA over Somali region. Figure 6 shows the distribution of sea-salt indirect effect (at the top of the atmosphere). In Figure 6 *a* cloud cover of 50% was assumed, whereas in Figure 7 the actual cloud cover was used.

For convenience the whole AS region has been divided into three sectors as follows:

(i) Sector A (50 to 75°E, 0 to 7.5°N); (ii) Sector B (52.5 to 72.5°E, 7.5 to 15°N); (iii) Sector C (60 to 70°E, 15 to 22.5°N).

Sector A extends over the southern AS, which covers the region of maximum wind speed and part of the Somali coastal region. Sector B extends over the central AS region, which also covers a part of the high wind speed region in the western AS during the summer monsoon. Sector C covers the northern part of AS.

Table 1 gives the average values of different parameters with their standard deviation for different sectors and seasons. Figures 4–6 show that regions of high winds have larger AOD and hence large forcing, both direct and indirect.

The most common feature observed is the increase in almost all the parameters as we proceed with time from FMA to JJA. The wind speed over AS slowly picks up and attains its maximum during the summer monsoon season and hence the highest values of forcing, since wind is the primary mechanism by which sea-salt aerosols are produced (we are considering only the wind generated aerosols) over this region. The indirect forcing

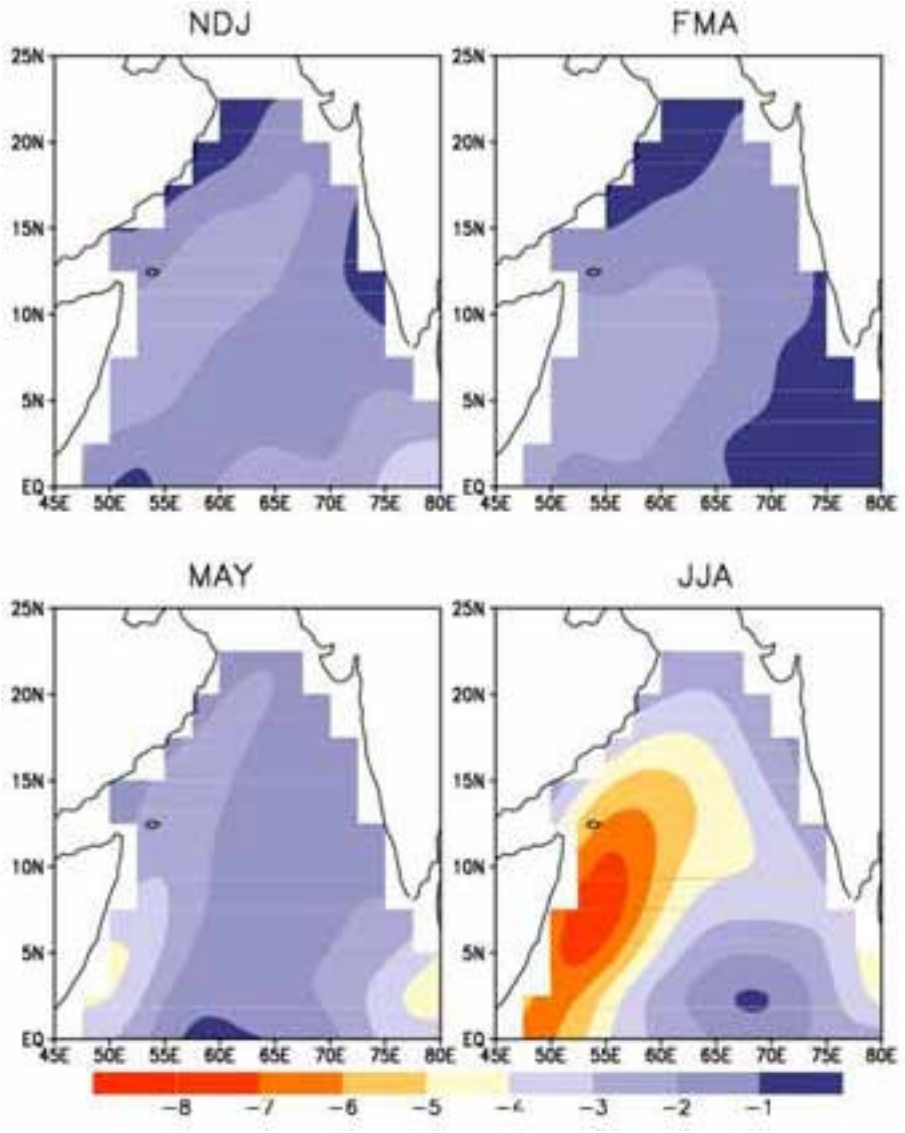

Figure 5. Estimated direct radiative forcing due to sea-salt aerosols over Arabian Sea during NDJ, FMA, MAY and JJA respectively.

Table 1. Aerosol parameters in different sectors over Arabian Sea

Parameter	Sector	NDJ	FMA	MAY	JJA
Sea-salt optical depth	A	0.046 ± 0.013	0.039 ± 0.017	0.052 ± 0.021	0.088 ± 0.047
	B	0.045 ± 0.013	0.043 ± 0.012	0.047 ± 0.012	0.112 ± 0.034
	C	0.035 ± 0.015	0.027 ± 0.012	0.041 ± 0.008	0.075 ± 0.024
Cloud optical depth	A	8.9 ± 1.0	8.1 ± 1.6	9.2 ± 1.4	11.0 ± 2.2
	B	8.7 ± 1.1	8.6 ± 1.0	8.9 ± 0.9	12.3 ± 1.3
	C	7.8 ± 1.5	6.9 ± 1.7	8.5 ± 0.6	10.6 ± 1.2
Direct radiative effect (Wm^{-2})	A	–1.95 ± 0.56	–1.63 ± 0.73	–2.19 ± 0.87	–3.71 ± 1.96
	B	–1.87 ± 0.54	–1.80 ± 0.50	–1.87 ± 0.54	–4.73 ± 1.44
	C	–1.45 ± 0.60	–1.13 ± 0.51	–1.74 ± 0.32	–3.13 ± 1.0
Indirect radiative effect* (Wm^{-2})	A	–14.2 ± 3.4	–14.8 ± 5.0	–15.4 ± 5.0	–22.8 ± 9.3
	B	–12.3 ± 2.1	–12.9 ± 3.4	–12.7 ± 2.4	–20.2 ± 6.6
	C	–11.27 ± 2.1	–14.28 ± 2.4	–8.64 ± 2.0	–14.28 ± 2.4

*Assuming a cloud cover of 50%.

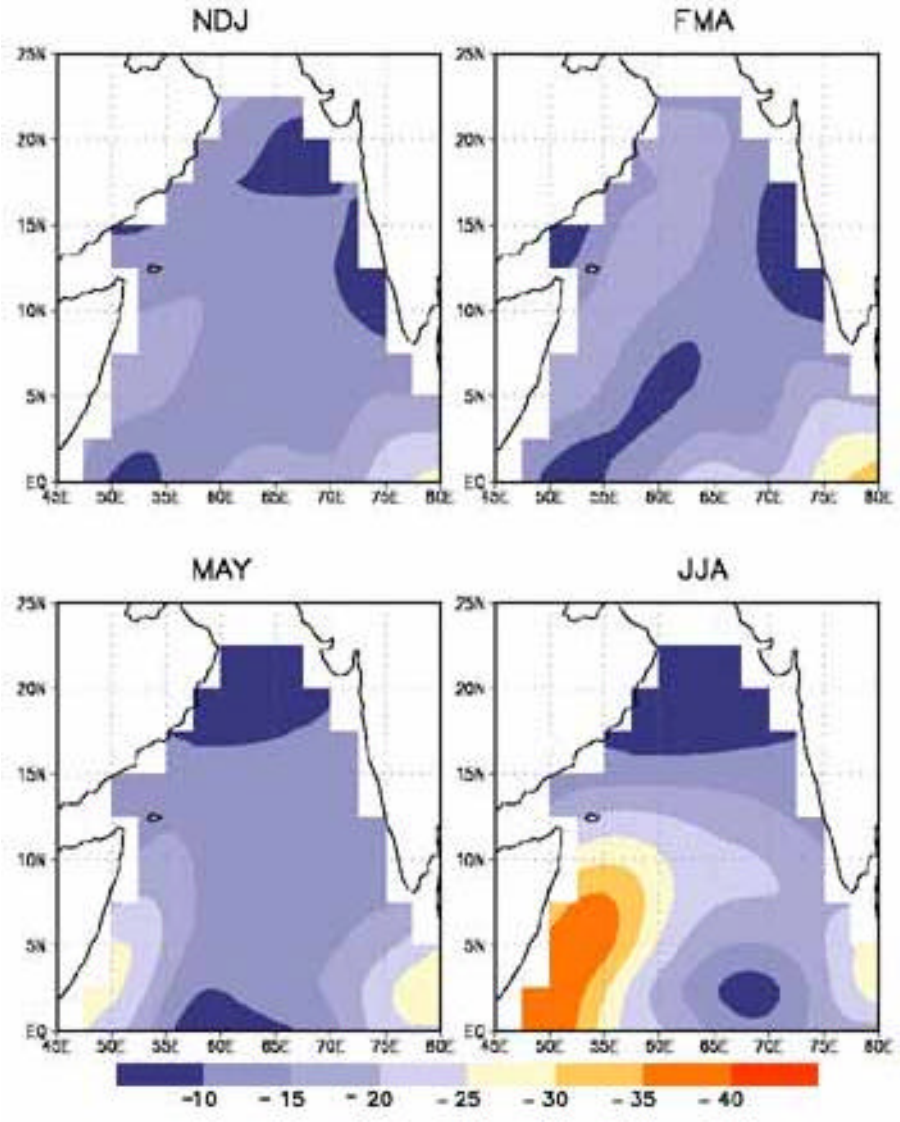

Figure 6. Estimated sea-salt indirect radiative forcing during FMA (Wm^{-2}) over Arabian Sea assuming 50% cloud cover.

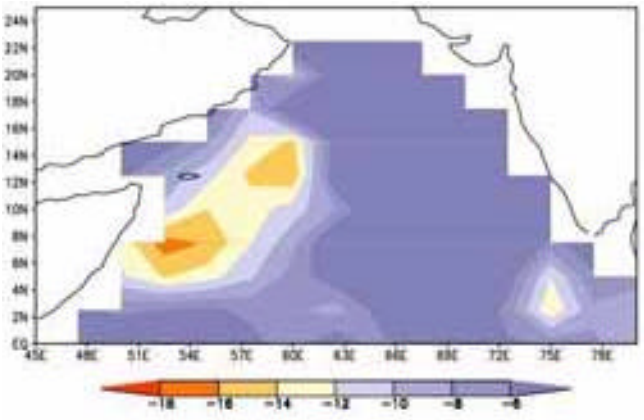

Figure 7. Estimated sea-salt indirect radiative forcing during FMA (Wm^{-2}) over Arabian Sea assuming the actual climatological cloud cover.

values shown in Figure 6 and Table 1 were calculated assuming a cloud cover of 50% over AS. When the actual cloud cover climatology over AS during FMA (when the INDOEX was conducted) was used from ISCCP (International Satellite Cloud Climatology Project) data, it was observed that the indirect forcing values were -6.91 ± 3.97, -6.98 ± 5.15 and -3.93 ± 3.32 Wm^{-2} over sectors A, B and C respectively. Regional distribution of sea-salt aerosol indirect forcing using actual cloud cover (ISCCP data) is shown in Figure 7.

The high winds observed during the summer monsoon season produce a large amount of sea-salt aerosols, thus resulting in high radiative forcing. It has been estimated that direct radiative forcing was as high as -4.73 Wm^{-2} during JJA. Indirect radiative forcing was observed to be as high as around -18 Wm^{-2} over the Somali coast region

in western AS. Similar values observed in almost all the parameters between sectors A and B, are due to the overlap of the Somali region (high wind speed region) in both the sectors. INDOEX studies reported values of indirect radiative forcing due to anthropogenic aerosols in the range –3 to –8 Wm^{-2} and direct radiative forcing in the range of –1 to –2 Wm^{-2}. The corresponding values of sea salt aerosol forcing in our study are larger than anthropogenic aerosols in this region, which brings out the importance of natural aerosols.

Caveats

(i) We have used the term 'indirect radiative forcing' due to sea-salt aerosols. Indirect forcing is generally defined as the indirect effect of an anthropogenic change to the natural aerosol distribution. So the term 'indirect radiative effect' may be more appropriate, since we discuss radiative impact of a natural aerosol species.

(ii) It should be noted that in our study the cloud cover is fixed. Thus the term 'indirect radiative forcing/effect' in this article represents modulation of the cloud radiative forcing due to the presence of sea-salt aerosols. In actual case, indirect radiative forcing depends on meteorology (such as vertical velocity) as well as its effect, which was not included in the present study due to the absence of data.

(iii) We have used average NCEP winds from 1995 to 2002. However, aerosol–cloud relationships used (eqs (6)–(9)) were derived from 1999 measurements. Similar data are not available for the other years. Our estimate of indirect radiative forcing for MAY and JJA is only indicative and may not be accurate. This is because eqs (6)–(9) were based on November–March observations.

Conclusions

The major conclusions are the following.

- Indirect forcing of sea-salt (natural) aerosol has been estimated for different seasons over AS.
- The results demonstrate the important role of wind speed on aerosol characteristics and hence its impact on direct and indirect radiative forcing.
- The magnitude of indirect radiative forcing (and uncertainty) due to sea-salt aerosols is several-fold more than the direct radiative forcing of sea-salt aerosols.
- The large magnitude and variability in both direct and indirect forcing due to sea-salt aerosols brings out the importance of natural aerosols over this region.

1. Twomey, S., Influence of pollution on short wave albedo of clouds. *J. Atmos. Sci*., 1977, **34**, 1149–1152.
2. Jones, A. *et al*., A climate model study of indirect radiative forcing by anthropogenic sulphate aerosols. *Nature*, 1994, **370**, 450–453.
3. Meehl, G. A. and Washington, W. M., El-Nino-like climate change in a model with increased atmospheric CO_2 concentrations. *Nature*, 1996, **382**, 60–65.
4. Jones, A. and Slingo, A., Predicting cloud-droplet effective radius and indirect sulphate aerosol forcing using a general circulation model. *Q. J. R. Meteorol. Soc*., 1996, **122**, 1573–1595.
5. Kogen, *et al*., Evaluation of sulphate aerosols indirect effect in marine stratocumulus clouds using observation-derived cloud climatology. *Geophys. Res. Lett*., 1996, **23**, 1937–1940.
6. Chuang, C. C. *et al*., Kinetic limitations on droplet formation in clouds. *Nature*, 1997, **390**, 594–596.
7. Le Treut, H. *et al*., Sulphate aerosol indirect effect and CO_2 greenhouse forcing: Equilibrium response of the LMD GCM and associated cloud feedbacks. *J. Climate*, 1998, **11**, 1673–1684.
8. Han, Q. Y., *et al*., Global survey of the relationships of cloud albedo and liquid water path with droplet size using ISCCP. *J. Climate*, 1998, **11**, 1516–1528.
9. Ramanathan, V. *et al*., Indian Ocean Experiment: An integrated analysis of the climate forcing and effects of the Great Indo-Asian haze. *J. Geophys. Res*., 2001, **106**, 28,371–28,398.
10. Kamra, A. K. *et al*., Background aerosol concentration derived from the atmospheric electric conductivity measurements made over the Indian Ocean during INDOEX. *J. Geophys. Res. – Atmos*., 2001, **106**, 28643–28651.
11. Moorthy, K. K. and Satheesh, S. K., Characteristics of aerosols over a remote island, Minicoy in the Arabian Sea: Optical properties and retrieved size characteristics. *Q. J. R. Meteorol. Soc*., 2000, **126**, 81–109.
12. Vinoj, V. and Satheesh, S. K., Measurements of aerosol optical depth over Arabian Sea during summer monsoon season. *Geophys. Res. Lett*., 2003, **30**, 1263, doi:10.1029/2002GL016664.
13. Woodcock, A. H., Salt nuclei in marine air as a function of altitude and wind force. *J. Meteorol*., 1953, **10**, 362–371.
14. Monahan, E. C., Sea spray as a function of low elevation wind speed. *J. Geophys. Res*., 1968, **73**, 1127–1137.
15. Saito, T. O., Yamada, K. and Nakaya, S., Chemical composition of oceanic aerosol. *J. Geophys. Res*., 1972, **77**, 5283–5292.
16. Exton, H. J., Latham, J., Park, P. M., Smith, M. H. and Allan, R. R., The production and dispersal of maritime aerosol. *Oceanic Whitecaps and Their Role in Air–Sea Exchange Processes* (eds Monahan, C. and Mac Niocaill, G.), Oceanic Sciences Library, D. Reidel, Dordrecht, 1986, pp. 175–193.
17. Parameswaran, K. *et al*., Effect of wind speed on mixing region aerosol concentrations in a tropical coastal environment. *J. Appl. Meteorol*., 1995, **34**, 1392–1397.
18. Moorthy, K. K., Satheesh, S. K. and Krishna Murthy, B. V., Investigations of marine aerosols over tropical Indian Ocean. *J. Geophys. Res*., 1997, **102**, 18,827–18,842.
19. Satheesh, S. K. *et al.*, Chemical, micro-physical and radiative properties of Indian Ocean aerosols. *J. Geophys. Res*., 10.1029/2002JD002463, 14 December 2002.
20. Satheesh, S. K. *et al.*, A model for the natural and anthropogenic aerosols for the tropical Indian Ocean derived from Indian Ocean Experiment data. *J. Geophys. Res*., 1999, **104**, 27,42127,440.
21. Prospero, J. M., Mineral sea salt aerosol concentrations in various ocean regions. *J. Geophys. Res*., 1979, **84**, 725–731.
22. Patterson, E. M. *et al*., Global measurements of aerosols in remote continental and marine regions: Concentrations, size distributions and optical properties. *J. Geophys. Res*., 1980, **85**, 7361–7376.
23. Taylor, J. P. and Mc Haffie, A., Measurements of cloud susceptibility. *J. Atmos. Sci*., 1994, 1298–1306.
24. Martin, G. M. *et al*., The measurement and parameterization of effective radius of droplets in warm stratocumulus clouds. *J. Atmos. Sci*., 1994, **51**, 1823–1842.

25. Snider, J. R. and Berenguier, J. L., Cloud condensation nuclei and cloud droplet measurements during ACE-2. *Tellus, Ser. B*, 2000, **52**, 828–842.
26. McFarquhar, G. M. and Heymsfield, A. J., Parameterizations of INDOEX micro-physical measurements and calculations of cloud susceptibility: Applications for climate studies. *J. Geophys. Res. – Atmos.*, 2001, **106**, 28675–28698.
27. Heymsfield, A. J. and McFarquhar, G. M., Microphysics of INDOEX clean and polluted trade cumulus cloud. *J. Geophys. Res. – Atmos.*, 2001, **106**, 28653–28673.
28. Ricchiazzi, P., Yang, S., Gautier, C. and Sowle, D., SBDART, A research and teaching tool for plane-parallel radiative transfer in the earth's atmosphere. *Bull. Am. Meteorol. Soc*., 1998, **79**, 2101–2114.
29. Hess, M., Koepke, P. and Schult, I., Optical properties of aerosols and clouds: The software package OPAC. *Bull. Am. Meteorol. Soc*., 1998, **79**, 831–844.

ACKNOWLEDGEMENTS. The study was carried out as part of ISRO–GBP and ARMEX. We thank Prof. J. Srinivasan, Centre for Atmospheric and Oceanic Sciences, Indian Institute of Science, Bangalore for valuable suggestions and guidance.

Received 17 October 2003; revised accepted 27 January 2004